Nonlinear intensity dependence in the infrared multiphoton excitation and dissociation of methanol pre-excited to different energies

Oleg V. Boyarkin, Thomas R. Rizzo, and David Rueda[a)]
Laboratoire de Chimie Physique Moléculaire, EPFL Ecublens, CH-1015 Lausanne, Switzerland

Martin Quack[b)] and Georg Seyfang
Physical Chemistry, ETH Zürich, CH-8093 Zürich, Switzerland

(Received 10 September 2001; accepted 27 June 2002)

We report quantitative dissociation yields for the reaction $CH_3OH\ (v_{OH}) \overset{nh\nu}{\rightarrow} CH_3 + OH$ induced by infrared multiphoton excitation of methanol pre-excited to various levels of the OH stretching vibration ($v_{OH}=0,1,3,5$). The yields are measured by detecting OH using laser induced fluorescence. It is demonstrated that for low levels of pre-excitation ($v_{OH}=0,1,3$) there is a substantial nonlinear intensity dependence, as a higher yield is found for self mode-locked CO_2 laser pulses (with higher peak intensity) as compared to single mode pulses of the same laser fluence, but lower peak intensity. In contrast, at high levels of preexcitation ($v_{OH}=5$) this nonlinear intensity dependence is absent. Quantitative model calculations are carried out using a case B/case C master equation approach that takes nonlinear intensity dependence into account. The calculations are consistent with the experimental results and confirm the prediction that an important part of the selectivity of the CO_2 laser excitation step in infrared laser assisted photofragment spectroscopy of CH_3OH is due to this nonlinear intensity dependence. We discuss further consequences of these experimental observations and theoretical predictions, which are also extended to infrared multiphoton excitation of C_2H_5OH. Infrared (C–O) chromophore band strengths are reported for CH_3OH and C_2H_5OH. [DOI: 10.1063/1.1501280]

I. INTRODUCTION

The nonlinear intensity dependence in multiphoton excitation has been a subject of discussion and investigation from the very start of the field.[1–4] Whereas in the multiphoton processes characteristic for visible and ultraviolet (UV) excitation of atoms and molecules one finds typically the nonlinearities expected from identifiable rate determining Göppert–Mayer or Shirley type transitions,[4] the simple rate equation treatments of stepwise multiphoton excitation and dissociation predict a linear intensity dependence for the rates of the individual transitions resulting in an (almost) pure fluence dependence of the overall excitation and dissociation product yields.[4–6] However, a more fundamental master equation treatment predicted nonlinear intensity effects in the stepwise multiphoton excitation of polyatomic molecules under certain conditions (case C of Ref. 7). This predicted nonlinear intensity dependence, as well as the intensity dependent transition between various regimes, was confirmed experimentally in a number of cases.[8–15] The phenomenon can now be modeled quantitatively with existing program packages.[16–18] It has been suggested to be of great importance in the design and optimization of infrared-laser isotope separation schemes.[19,20]

Infrared laser assisted photofragment spectroscopy (IRLAPS) is a new application of infrared (IR) multiphoton excitation for molecular spectroscopy.[21–23] Briefly, it consists in preexciting molecules via a spectroscopic transition to some high rovibrational level and then in detecting the pre-excited molecules selectively by subsequent infrared multiphoton excitation, dissociation, and observation of the photofragments. The high selectivity for pre-excited molecules, which is needed in order to have a useful discrimination against multiphoton excitation and dissociation of ground-state molecules[21–23] has its origins in three main effects:[24]

(i) The multiphoton excitation of pre-excited molecules is carried out with an infrared (CO_2) laser tuned to the low wave number side of the fundamental transition, because typically even the one-photon infrared maximum absorption of the pre-excited molecules is shifted to lower wave number;
(ii) multiphoton dissociation of the pre-excited molecules requires a lower fluence, even in the linear regime of multiphoton excitation (case B);[7]
(iii) because the pre-excited molecules are carried to energy regimes of much higher effective densities of states which are coupled by intramolecular vibrational redistribution (IVR[25]), the case C→case B transition as a function of initial excitation will lead to much less stringent intensity requirements for IR multiphoton dissociation of small molecules.

It has been suggested[24] that the last effect is particularly important for the selectivity of IRLAPS of small molecules such as methanol, and this could be tested by examing the

[a)]Visiting diploma thesis fellow ETH Zürich.
[b)]Author to whom correspondence should be addressed. Fax: ++41-1-632 10 21; Telephone ++41-1-632 44 21. Electronic mail: martin@quack.ch

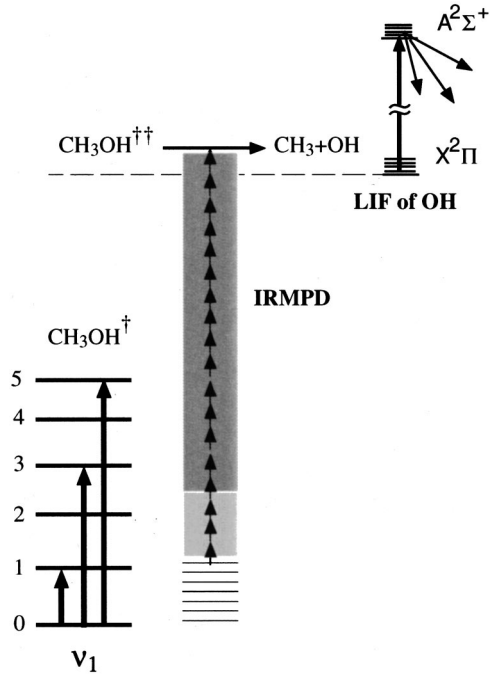

FIG. 1. Level scheme for IR laser assisted photofragment spectroscopy (IRLAPS) of CH_3OH.

intensity dependence. This suggestion has received further attention in relation to two step isotope separation schemes,[26] which might be optimized by making use of the nonlinear intensity dependence.

It is the aim of the present paper to address the question of the nonlinear intensity dependence in the multiphoton excitation of preexcited molecules both experimentally and by comparison with theoretical simulations. As a test molecule we have selected methanol using the scheme

$$CH_3OH \xrightarrow{h\nu} CH_3OH^* \xrightarrow{nh\nu'} CH_3 + OH. \quad (1)$$

We have studied the infrared multiphoton dissociation yields of vibrational ground-state methanol as well as methanol preexcited to various vibrational levels of the OH stretching mode as detailed in Fig. 1 ($v=0,1,3,5$). Our study clearly establishes a pronounced nonlinear intensity dependence on the selectivity of IRLAPS.

II. EXPERIMENT

Figure 1 shows a schematic energy level diagram for the IRLAPS process of CH_3OH. In the IR multiphoton excitation experiments of vibrationally excited methanol, we first excite the molecules from the vibrational ground state to the $v_{OH}=3$ or $v_{OH}=5$ OH stretching vibrational overtone levels by the output of a pulsed (6 to 7 ns pulse duration) dye laser or to the $v_{OH}=1$ level by an infrared pulse generated by difference frequency mixing (DFM). Approximately 100 ns after the preparation pulse, the preexcited molecules are dissociated by a pulsed TEA–CO_2 laser in an infrared multiphoton absorption process. The OH fragments from the unimolecular dissociation of CH_3OH are detected by a third (UV) laser pulse via laser induced fluorescence (LIF) ~700 ns after the preparation pulse. The dissociation yields of the

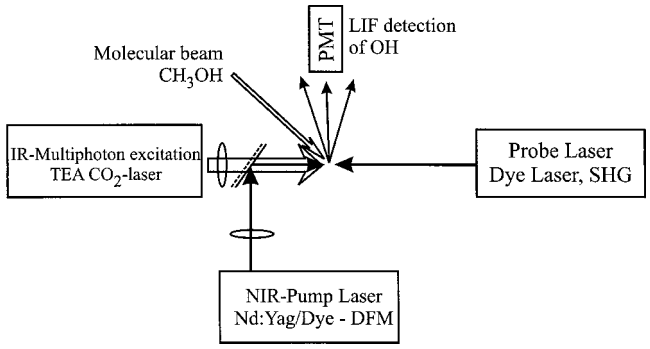

FIG. 2. Schematic drawing of the experimental setup for IRLAPS of CH_3OH (see discussion in the text).

IR multiphoton excitation process are monitored by the total LIF signal. To measure the dependence of the dissociation yield on CO_2 laser fluence, the pulse energy is attenuated by a set of calibrated CaF_2 and BaF_2 windows. In order to investigate the nonlinear intensity dependence of the IR multiphoton excitation process, the CO_2 laser is operated in two different regimes. In the free running regime, the laser is self mode-locked (with pulse to pulse fluctuations in the locking efficiency), and its output consists of short high intensity spikes (pulse width less than 1.6 ns [full width at half maximum (FWHM)] under ideal locking conditions). By inserting an intracavity absorber,[12] we force the laser to run in the single mode regime where the laser pulse is smooth and reproducible in time (~150 ns FWHM for the initial peak), showing no high intensity spikes. Thus, operating the laser in the two different regimes we can change the peak intensity of the IR laser field independent of the laser fluence.

A simplified scheme of the experimental apparatus is shown in Fig. 2. The experimental setup has been described in detail elsewhere.[27] To excite the OH-stretching fundamental of jet-cooled CH_3OH about 1 mJ of IR radiation around 3570 cm^{-1} is generated by difference frequency mixing (DFM) the output of a Nd:YAG pumped dye laser (Spectra Physics GCR-270, Lambda Physics Scanmate) with the fundamental of the same Nd:YAG laser in a $LiNbO_3$ crystal. Overtone excitation of methanol to $v_{OH}=3$ at about 10 530 cm^{-1} and $v_{OH}=5$ at about 16 750 cm^{-1} is accomplished by the output of another dye laser (Lumonics HD 500) which is Raman shifted in H_2 to generate 10 530 cm^{-1} radiation and which is pumped by the same Nd:YAG laser. We produce ~9 mJ/pulse at 10 530 cm^{-1} and 60 mJ/pulse at 16 750 cm^{-1} within a laser line width of 0.05 cm^{-1} to excite these two bands. At this width the laser light overlaps several rotational transitions in each band. The output of a third Nd:YAG pumped dye laser (Quantel YG-681G, Quantel TDL51) is frequency doubled to 32 474.4 cm^{-1} and used to probe vibrational ground-state OH in the $J=1$ level via LIF in the $A-X$ band.[28] All wavelengths of the dye lasers are calibrated and verified by a pulsed wavemeter (Burleigh WA-4500).

A TEA–CO_2 laser (Lumonics TEA 841) is used for the IR multiphoton excitation of methanol molecules. It is operated in the unstable resonator mode and is capable of delivering energies up to 1.2 J per pulse in a low divergence beam. In all our experiments this laser is tuned to the

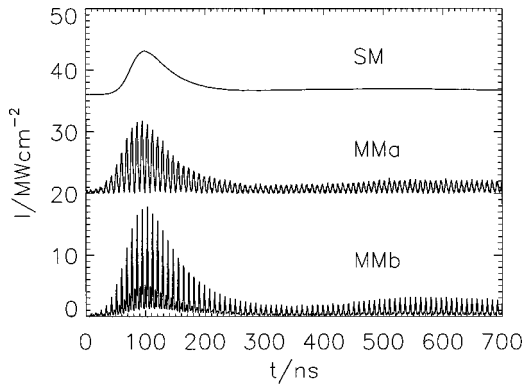

FIG. 3. CO_2 laser pulse shapes for the IR multiphoton excitation of CH_3OH. The laser intensity is given for a nominal laser fluence of $F = 1.0\ J\,cm^{-2}$. Upper trace: Single mode pulse (SM), lower trace: Multimode pulse (MM_b) with nearly identical phases for most of the longitudinal resonator modes, middle trace: Multimode pulse with less favorable phase distribution (MM_a).

10P(20) line at 944.19 cm^{-1}, which is shifted to low wave number from the ν_8 CO-stretching fundamental absorption of CH_3OH (1033.5 cm^{-1}).

Without any modifications, the CO_2 laser operates in the self mode-locked regime. The overall pulse shape of this self mode-locked laser consists of an initial peak of 150 ns containing 35% of the pulse energy followed by a 5 μs tail carrying the remainder of the energy. We arrange the timing of our experiment to use the initial peak by detecting only the dissociation products that are produced during the first 600 ns of the CO_2 laser pulse. As depicted in Fig. 3 close examination with a fast photon drag or pyroelectric detector (time resolution <0.5 ns) shows that the pulse shape has a significant fine structure. The pulse consists of a train of spikes shorter than 1.6 ns (FWHM) which are separated by the 8 ns round trip time of the cavity. Under less favorable conditions the peaks are broadened or split in two or even three spikes. This pulse shape is typical for partially mode-locked lasers. We use an intracavity absorber to make this laser run on a single longitudinal mode. The technique has been described in detail elsewhere.[29] A 10 cm long aluminum cell, fitted with sodium chloride Brewster windows, is inserted into the CO_2 laser cavity and filled with a few mbar of SF_6 gas. The spectrum of SF_6 overlaps with some of the 10P CO_2 laser transitions. By adjusting the pressure of the intracavity absorber, conditions may be found where all the longitudinal modes except the strongest are suppressed, and the lasing occurs on this single longitudinal mode. A weak flow of SF_6 through the intracavity cell is recommended to obtain stable, long term single mode operation of the laser. The overall shape of the single mode pulse is similar to the envelope of the multimode (self mode-locked) pulse including the long 5 μs tail, but it does not show any spikes. Figure 3 shows three different laser pulses: a single mode pulse (upper trace), a ''typical'' multimode pulse, in which the individual peaks are significantly broadened (middle trace), and an almost ideally locked multimode pulse with nearly identical phases for most of the longitudinal resonator modes (lower trace). For a laser fluence of 1.0 $J\,cm^{-2}$ within the first 600 ns—the part of the CO_2 laser pulse that has been used in the experiments—the maximum intensity for these laser pulses is 7.2, 11.7, and 17.9 $MW\,cm^{-2}$, respectively.

A solenoid actuated pulsed valve with 0.5 mm diameter orifice expands a mixture of 40 mbar methanol in about 2.0 bar of helium into a stainless steel vacuum chamber evacuated by a 6-inch diffusion pump. The average pressure in the chamber with the pulsed jet operating is $\sim 5\times 10^{-6}$ mbar. We estimate the rotational temperature of the molecules in the expansion to be between 4 and 8 K based on simulations of the rovibrational band contour. Approximately 10 mm downstream from the nozzle, the free jet expansion is crossed either by the IR beam for the excitation of the v_{OH} fundamental vibration or by the dye laser beam for overtone excitation. All the laser beams for preexcitation are focused by 50 cm focal length CaF_2 lens. The CO_2 laser crosses the free jet slightly downstream from the preexcitation. This beam is focused by a 1 m focal length Ge lens and counterpropagates with respect to the pump beam. The UV probe laser beam is gently focused with 1 m focal length fused silica lens and is combined with the preexcitation beam using a dichroic mirror. The probe beam propagates parallel to the pre-excitation beam but is offset by ~ 1 mm downstream to compensate the displacement of the molecules in the jet during the delay between the pump and probe laser pulses. The spatial profiles of all the beams at the focus were measured by monitoring the laser power through a small slit (width 20 μm for the dye laser and 50 μm for the IR beam) as a function of the slit position. The measured widths (FWHM) are ~ 600 μm for the IR beam, 200 μm for the dye beam and 400 μm for the UV and CO_2 laser beams. This distribution of beam sizes limits somewhat the exact absolute definition of fluences, although the relative changes of fluence are well defined. The CO_2 laser beam from the unstable resonator optics in these experiments is almost Gaussian close to the focus, with somewhat extended wings. In principle the experiments convolute the various beam profiles.

A 50 mm focal length $f/1$ fused silica condenser lens collects the fluorescence from the OH fragments and images it onto a 2 mm wide slit in front of a UV sensitive photomultiplier tube (EMI 9635QB). The resulting signal is sent to a gated integrator (LeCroy 2249SG), digitized and transferred to a 80 486 computer via a computer aided control interface (CAMAC). We operate the CO_2 laser at 10 Hz and the pump and probe laser at 20 Hz, subtracting the background from the scattered probe laser light on alternative shots. Each data point typically represents an average of 100–150 laser shots.

The relative CO_2 laser output energy is measured by means of a pyroelectric film detector with an active area of $10\times 10\ mm^2$. The linearity of this detector within the range of the applied CO_2 laser pulse energy was carefully checked using several CaF_2 and BaF_2 windows, the transmittance of which was measured with a FTIR spectrometer. The absolute value of the CO_2 laser output is determined by a calibrated power meter (Scientech-AC 5002H). The absolute fluence in the experiments is determined to within about 30% uncertainty, however the relative fluences, which are relevant for comparing a set of experiments, are much more accurate (a few percent uncertainty at most). The *spatial* fluence distri-

butions were not simulated in detail in the calculations reported below, but were represented by one characteristic fluence.

At high CO_2 laser fluence, we unavoidably dissociate a small fraction of ground-state CH_3OH by infrared multiphoton excitation alone. To obtain the dissociation yield of only the vibrationally excited molecules we first obtain dissociation yields from the ground and vibrationally excited state together. Then, in a control experiment we block the dye laser (or DFM) beam to the measure the dissociation yields from only ground-state molecules. The true dissociation yields for pre-excited CH_3OH are then obtained by subtraction. The corrections usually are on the order of a few percent and may increase to 10% under unfavourable conditions.

For modeling the infrared multiphoton excitation, integrated band strengths were derived from quantitative measurements of IR absorption of CH_3OH and C_2H_5OH. To determine the IR absorption cross section for CH_3OH and C_2H_5OH, in the region of the CO_2-laser emissions, infrared spectra have been recorded between 800 and 1500 cm^{-1} using a FTIR spectrometer (Bomem DA.002) and a conventional grating IR spectrometer (Perkin Elmer G983). In the FTIR spectrum (apodized instrumental bandwidth: 0.004 cm^{-1} FWHM), the rotational structure of CH_3OH could be resolved, whereas the spectra from the grating spectrometer were limited by the spectral resolution of 0.5 cm^{-1}. To avoid distortions in the measured IR absorption cross section, the spectra were collisionally broadened by adding 1 bar of N_2. The rotational structure could not be resolved for C_2H_5OH, even at the highest resolution.

III. THEORY

A. Master equation treatment of IR multiphoton excitation including nonlinear intensity dependence

In principle, one might consider quantum dynamical modeling of infrared multiphoton excitation in the quasiresonant or Floquet (classical periodic field) approximations.[7,16,30] Such attempts (including rotation) have been made for very simple molecules such as ozone[31,32] or recently hydrogen fluoride.[33] For molecules like methanol such an approach is still impractical even today, as the spectroscopic states are still not sufficiently characterized and the total density and number of rovibrational states to be included in a simulation would be far too large. However, the relatively large number of rovibrational states renders the statistical case B/C master equation treatment a satisfactory approximation. In this treatment one solves the differential equation for the coarse grained energy level populations[7,30]

$$\frac{d\mathbf{p}}{dt} = \mathbf{K}\mathbf{p}. \tag{2}$$

In contrast to ordinary rate equation treatments with Einstein coefficients for absorption and stimulated emission that depend linearly on intensity, this treatment includes nonlinear intensity dependence.[7,30,34,35] The off diagonal elements $K_{M+1,M}$ and $K_{M,M+1}$ of the coefficient matrix K will in general depend nonlinearly on the laser intensity I (case C). For the special case of a linear intensity dependence (case B), a simplified model for the up-pumping rate can be used

$$K_{M+1,M} = 1.511 \cdot \frac{(G_{Ch}/pm^2)(I/\mathrm{MW\,cm^{-2}})\rho_M^{0'}}{(\Delta\nu/\mathrm{cm^{-1}})\rho_M}, \tag{3}$$

where G_{Ch} is the integrated band strength for the pumped chromophore transition (see Sec. IV B), I is the laser intensity, ρ_M is the density of the effectively coupled states at level M (in general the density for all vibrational degrees of freedom is used in the calculations), $\rho_M^{0'}$ is the density of states where the degree of freedom corresponding to the pumped vibration—here the CO-stretching vibration—has been removed from the count. Equation (3) contains one adjustable parameter, the effective coupling width $\Delta\nu$. In the model calculations for CH_3OH $\Delta\nu = 325\ cm^{-1}$ is used. It is determined by adjusting the calculated dissociation yields F_P to the experimental results for pre-excitation to $v_{OH} = 3$.

The diagonal terms of the coefficient matrix K are given by

$$-K_{M,M} = k_M(E) + \sum_{N \neq M} K_{N,M}, \tag{4}$$

where the specific unimolecular decay rate coefficient $k_M(E)$ ($k_M = 0$ for $E < E_0$) accounts for the dissociation of highly excited CH_3OH into CH_3 and OH from level M. The unimolecular rate coefficient may be calculated from statistical theory

$$k_M(E) \simeq k(E,J) = \gamma \cdot \frac{W(E,J)}{h\rho(E,J)}, \tag{5}$$

assuming a transmission coefficient $\gamma = 1$. The number of open reaction channels W has been determined applying Rice–Ramsperger–Kassel–Marcus (RRKM) theory and neglecting the dependence of the rate constants upon angular momentum J (see the review[36] and references cited therein). The vibrational density of states $\rho(E)$ for the reactant and the activated complex has been calculated by a direct anharmonic counting mechanism based on the Beyer–Swinehart algorithm using convolution with anharmonic densities.[37–39] Most of the normal vibrations have been treated as harmonic oscillators and the frequencies have been taken from Ref. 40. The torsional mode has been treated separately (see Sec. III B). Morse oscillators have been used to model the CH- and OH-stretching vibrations as well as the reactive CO-stretching vibration. $D_0(CH) = 34\,000\ cm^{-1}$ and $D_0(OH) = 37\,000\ cm^{-1}$ have been chosen as effective dissociation energy parameters for the Morse potential. The dissociation energy $D_0(CO)$ has been adjusted to reproduce the experimentally determined Arrhenius parameter of $A_\infty = 9.4 \cdot 10^{15}\ s^{-1}$ and $E_{A\infty} = 374\ kJ\,mol^{-1}$ for the dissociation of CH_3OH into CH_3 and OH.[41]

It is clear that the present treatment of unimolecular dissociation of methanol is very crude, and for a simple bond fission reaction the statistical adiabatic channel model would be more appropriate.[36,42] However, it is known that multiphoton excitation rather than the unimolecular dissociation step is rate determining and therefore rough approximations

can be accepted in the statistical treatment for the dissociation of methanol, as long as product state distributions are not required.[4,36]

In the limiting case of linear intensity dependence of the IR multiphoton excitation process, the down pumping rate $K_{M,M+1}$ is calculated from the relaxed population distribution.[7,30,34,35]

$$K^{(B)}_{M,M+1} = K_{M+1,M}\frac{p^{\mathrm{rel}}_M}{p^{\mathrm{rel}}_{M+1}} = K_{M+1,M}\frac{\rho_M}{\rho_{M+1}}. \tag{6}$$

Nonlinear intensity effects have been included in the model by correcting the down pumping rate $K_{M,M+1}$ by a correction factor[35] $f^C_{M,M+1} \sim I^{-1/2}$

$$K^C_{M,M+1} = f^C_{M,M+1} K^B_{M,M+1}, \tag{7}$$

$$f^C_{M,M+1} = \left(\frac{\pi\sqrt{3}}{2}|V_{M+1,M}|\rho_{M+1}\right)^{-1}, \tag{8}$$

where $V_{M,M+1}$ is the effective coupling matrix element between the adjacent level M and M+1.[7,35] In practical calculations, Eq. (9) is used for the transition from a nonlinear (case C) to a linear intensity dependence (case B) of the IR multiphoton excitation process due to an increased laser intensity or to excitation of the molecules to higher levels

$$K^{B,C}_{M,M+1} = \max\{K^B_{M,M+1}, K^C_{M,M+1}\}, \tag{9}$$

where $\max\{x,y\}$ is the larger quantity of x and y.

B. Treatment of the OH torsional mode

To investigate in more detail the influence of the treatment of the OH-torsional mode on the IR multiphoton excitation process, three different models have been compared. In a first approximation, a harmonic oscillator with $\tilde{\nu}_0 = 272.5\ \mathrm{cm}^{-1}$ has been assumed for the $0 \rightarrow 1$ transition of the torsional vibration. Another limiting case to consider is the free rotation of the H atom about the CO-axis relative to the methyl group. From the published structural data, a rotational constant $B_{\mathrm{tor}} = 26.171\ \mathrm{cm}^{-1}$ is determined for this rotation.[40] As discussed in Ref. 39, a more accurate method interpolating between these two limiting cases is to solve the Schrödinger equation for the separated torsional mode on a grid and to calculate the exact energy eigenvalues for this degree of freedom.[39,43–47] With an effective rotational constant F for the torsional motion, the Hamiltonian is given by

$$H_{\mathrm{tor}} = -F\partial^2/\partial\gamma^2 + V(\gamma), \tag{10}$$

$$V(\gamma) = \frac{V_3}{2}(1-\cos 3\gamma) + \frac{V_6}{2}(1-\cos 6\gamma). \tag{11}$$

The potential constants $V_3 = 373.21\ \mathrm{cm}^{-1}$ and $V_6 = -0.52\ \mathrm{cm}^{-1}$ were taken from Ref. 40 (but see also Refs. 48 and 49). The coupling of the torsion to other modes, in particular the dependence of the effective torsional barrier upon OH-stretching excitation, is important,[46,48] but is neglected here. The calculated energy eigenvalues for the three different models are shown for $E_{\mathrm{tor}} \leqslant 1500\ \mathrm{cm}^{-1}$ in Fig. 4. The eigenvalues for the exact calculation are labeled with symmetries according to the point group C_{3v} where the levels with E-symmetry are twofold degenerate. There is a significant difference for the hindered rotor and the free rotor assumption only for the lowest eigenvalues. For higher excitations of the torsional mode, the two descriptions are equivalent (see left and middle column in Fig. 4) and give a significantly lower density of states compared to the harmonic oscillator model, whose level energies are systematically below the corresponding level energies of the other models for the higher excitations (see right hand column in Fig. 4). Also included in Fig. 4 is the correlation between equivalent energy eigenvalues for the different models. Figure 5 shows the resulting total densities of states for the three models.

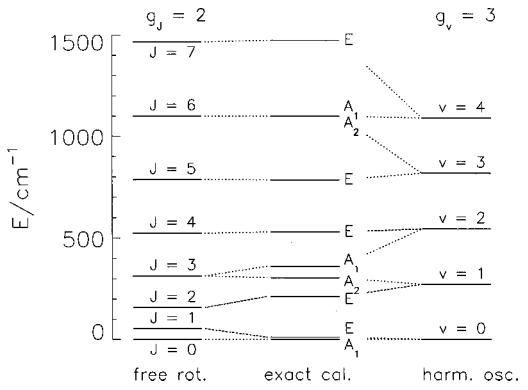

FIG. 4. Lowest energy levels for different treatments of the OH-torsional mode in CH_3OH. The dotted line represents the correlation between equivalent energy eigenvalues for the different models (note the different degeneracies $g_J = 2$ in the rotational, except for $J = 0$, and $g_v = 3$ in the vibrational model for the levels).

For the IR multiphoton excitation of CH_3OH, the level of transition from a case C description to case B behavior corresponding to Eq. (9) is shown as function of laser intensity in Fig. 6. Of the different models used to describe the OH-torsional mode, the harmonic oscillator approximation gives the lowest level for the transition to a linear intensity dependence of the IR multiphoton excitation process, as expected from the higher density of states for $E > 700\ \mathrm{cm}^{-1}$

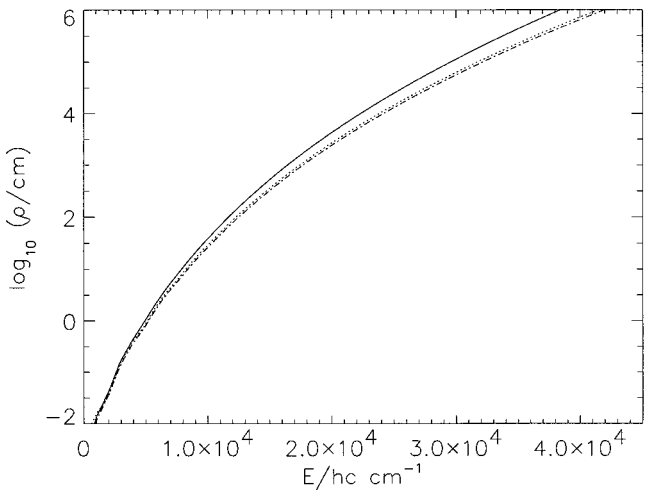

FIG. 5. Calculated vibrational density of states for CH_3OH for the different models to describe the torsional mode: (——): harmonic oscillator, (— · — · —): free rotor (· · · ·): exact calculations using the Hamiltonian of Eqs. (10) and (11).

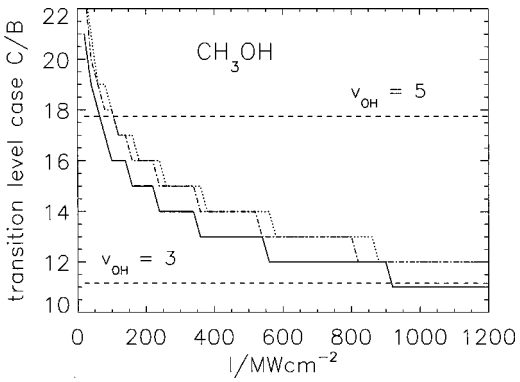

FIG. 6. Level of transition of a case C to a case B behavior as a function of CO_2 laser intensity according to Eq. (9) for the IR multiphoton excitation of CH_3OH. Three different models have been used to describe the OH-torsional mode. ——: harmonic oscillator, (—·—·—·—): exact, (· · · ·): free rotator using the Hamiltonian of Eqs. (10) and (11). Also included in the plot are the excitation energies (— — —) for $v_{OH}=3$ and $v_{OH}=5$.

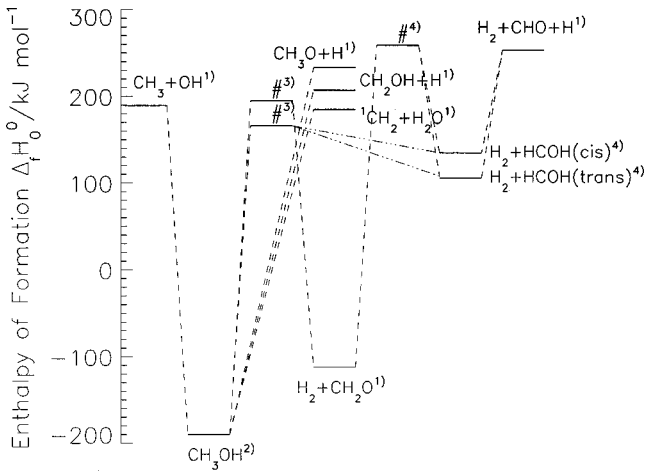

FIG. 7. Energy diagram for different unimolecular reaction channels of CH_3OH. References for the thermochemical data. Refs. 53[3)], 54[1)], 85[2], and 86[4] (not zero-point energy corrected).

(see Fig. 5). From the intensity dependence of the level for a transition to case C behavior, it may be concluded that only small or even no nonlinear intensity effects are expected for the IR multiphoton excitation of CH_3OH pre-excited to $v_{OH}=3$ or to $v_{OH}=5$.

C. Unimolecular dissociation channels for CH_3OH and calculated product distribution

Because we probe only the OH reaction product after IR-multiphoton dissociation of methanol, we must determine whether the number of detected OH-radicals accurately reflects the dependence of the total IR multiphoton excitation and dissociation rates on laser parameters. The question of the different unimolecular reaction channels has been already addressed in early IR multiphoton excitation experiments on methanol.[50,51] The potential hypersurface of CH_3OH allows for a large variety of possible channels for an excitation energy around 380 kJ mol^{-1}. High level *ab initio* calculations using CASSCF gradient methods,[52,53] together with published thermochemical data, prove six different reaction channels for an excitation energy between 355 and 430 kJ-mol, as summarized in Table I.

A correlation diagram for the different reaction channels is shown in Fig. 7.

The reaction channel leading to CH_3- and OH-radicals has been studied and well characterized in shock tube experiments,[41] which give an Arrhenius activation energy of 374 kJ mol^{-1} and a pre-exponential factor of $A=9.4 \cdot 10^{15}$ s^{-1}. As ~30 additional CO_2 laser photons have to be absorbed to break the C–O bond in HCOH or CH_2OH,[54] we assume that the OH-radicals detected by LIF result exclusively from the unimolecular dissociation of multiphoton excited CH_3OH. Consecutive IR multiphoton excitation and dissociation of highly excited formaldehyde is conceivable, leading to $CO+H_2$.[55]

TABLE I. Reaction channels for methanol decomposition.

Reaction No.	Product	Threshold energy	Ref.
1.	$CH_3OH \rightarrow CH_3+OH$	$\Delta_r H_0^0=377.2$ kJ mol^{-1}	54
2.	$\rightarrow H_2+H_2CO$	$E_A=384.6$ kJ mol^{-1}	53
3.	$\rightarrow H_2+HCOH$	$E_A=355.7$ kJ mol^{-1}	53
4.	$\rightarrow {}^1CH_2+H_2O$	$\Delta_r H_0^0=377.5$ kJ mol^{-1}	54 and 82
5.	$\rightarrow CH_2OH+H$	$\Delta_r H_0^0=395.3$ kJ mol^{-1}	83
6.	$\rightarrow CH_3O+H$	$\Delta_r H_0^0=430.5$ kJ mol^{-1}	84

Further reaction channels have been investigated through bimolecular reaction of electronically excited $O(^1D_2)$ with CH_4[56–58] or through the recombination reaction of CH_3 with OH.[59] Hack and Thiesemann determined CH_2O, $^1CH_2$, OH and ground state $O(^3P)$ from the unimolecular dissociation of chemically activated CH_3OH by LIF.[56] At an excitation energy of 559 kJ mol^{-1} with respect to the vibrational ground state of CH_3OH, they found that the unimolecular decay process is dominated by the OH-channel (90%) whereas the other decay channels are of minor importance: 6% for CH_2O, 2% for $^1CH_2$ and for $O(^3P)$. Humpfer *et al.* investigated the bimolecular reaction of CH_3 with OH in a flow reactor at 700 K and a total pressure of 65 Pa.[59] For the reaction channels leading to HCOH, $^1CH_2$ and CH_2O they determined a ratio for the rate constants of 1.00:0.82:0.15. Lin *et al.* studied the reaction of electronically excited $O(^1D_2)$ with CH_4 in crossed molecular beams.[57] They concluded that CH_2OH, CH_2O and HCOH are formed through a long-lived complex, while for the CH_3+OH channel a direct H-atom abstraction pathway is clearly more important than the pathway via a long lived $(CH_3OH)^*$ intermediate. The assumption of different reaction pathways for the CH_3+OH channel was confirmed recently in time resolved femtosecond experiments where the $CH_4 \cdot O_3$ van der Waals complex was used as a precursor for $O(^1D_2)$ and the OH-radicals were detected by laser induced fluorescence.[58] Finally Brouard *et al.* have interpreted product state distributions from $O(^1D_2)+CH_4$ to indicate nonstatistical energy distributions in the intermediate complex $(CH_3OH)^*$[60] although their analysis has been subject to questions.[61,62]

The calculated transition state structures[53] and available thermochemical data[41,54] have been used to calculate $k(E)$

for reaction channels (1)–(6) in Table I. A comparison of the calculated $k_i(E)$ for the reactions (2)–(4) with the experimental results from Humpfer *et al.*[59] clearly shows that the calculated $k_3(E)$ is significantly too large. To get a better agreement between experiment and theory the calculated vibrational frequencies at the transition state for reaction (3) have been modified to reduce the preexponential Arrhenius factor $A_{3\infty}$ determined for $T=700$ K by a factor of 3. With this slight modification a unimolecular dissociation rate constant

$$k_{\mathrm{tot}}(E)=\sum k_i(E), \tag{12}$$

for CH_3OH including all reaction pathways is calculated and introduced into the master equation for the IR multiphoton excitation and dissociation. At the time t_P of the UV-probe pulse the reaction yields $F_{P,i}$ for the different product channels are calculated from

$$F_{P,i}(t_P)=\sum_M p_M(t_p)\frac{k_i(E_M)}{k_{\mathrm{tot}}(E_M)}, \tag{13}$$

where the p_M are the time integrated (until t_p) relative populations of all products levels at an excitation energy E_M. The relative reaction yields $F'_{P,i}$ for a given product channel i at the time t_P are determined from

$$F'_{P,i}=F_{P,i}/\sum_j F_{P,j}=F_{P,i}/F_{P,\mathrm{tot}}. \tag{14}$$

For the multiphoton excitation of CH_3OH preexcited to $v_{OH}=3$ the relative reaction yields $F'_{P,OH}$ for the OH-dissociation channel have been calculated for different CO_2 laser fluences. It increases only slightly from $F'_{P,OH}=0.48$ for $F=15\ \mathrm{J\,cm^{-2}}$ ($F_{P,\mathrm{tot}}=0.05$) to $F'_{P,OH}=0.63$ at $F=75\ \mathrm{J\,cm^{-2}}$ ($F_{P,\mathrm{tot}}=0.97$). As the relative product yields $F'_{P,i}$ depend to a very good approximation only on the rate coefficients $K_{MN}(E)$ around and above the reaction threshold (where case C effects are negligible) and on the relative size of the $k_i(E)$ for the individual reaction channels, the calculated $F'_{P,i}$ are independent on the degree of preexcitation. Thus the measured LIF-signal for OH gives a reliable measure to determine the dependence of the total dissociation yields $F_{P,\mathrm{tot}}$ on the degree of preexcitation, laser intensity and laser fluence for the IR multiphoton excitation of CH_3OH. Using a constant proportionality factor, the corrections at the extrema would be about $\pm 10\%$ and have been neglected in our analysis, although they could be introduced, if desired.

Another correction would arise from the change of the OH rotational distribution with the CO_2 laser intensity. A higher intensity of the CO_2 laser will lead to a higher average energy of the dissociating molecules and thus, in a statistical model for the product state distribution, also to a higher average rotational excitation of the product OH. Again this correction could be introduced at considerable expense using statistical models for product state distributions.[36,39,55,63,64] However, the corrections are expected to be sufficiently small (and uncertain) as to not be warranted, as they would not, in any case, change the conclusions reported below.

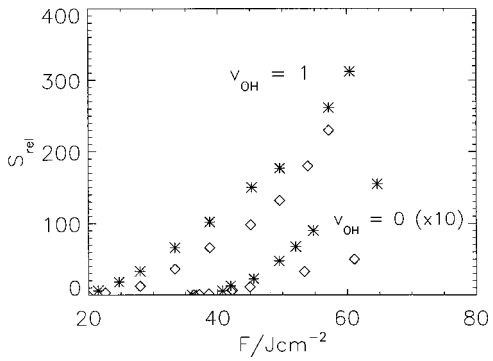

FIG. 8. Measured OH fluorescence signal as a function of CO_2 laser fluence for the IR multiphoton dissociation of CH_3OH from the vibrational ground state and preexcited to $v_{OH}=1$. The LIF signal for the dissociation from the ground state is multiplied by a factor of 10. (*): multimode pulse, (◇): single mode pulse.

IV. RESULTS AND DISCUSSION

A. Measured dissociation yields for different levels of pre-excitation of CH_3OH

The dissociation yields after IR multiphoton excitation have been determined for CH_3OH in the ground state and pre-excited to the $v=1$, 3, and 5 level of the OH-stretching vibration. As a shift of the maximum absorption of the pre-excited molecules towards lower wave numbers is expected, the 10P20 CO_2 laser line at 944.194 $\mathrm{cm^{-1}}$ has been chosen to improve the selectivity of the IRLAPS experiments. This line is shifted nearly 100 $\mathrm{cm^{-1}}$ to lower wave numbers compared to the band center of the CO-stretching vibration (ν_8)[40] at 1033.5 $\mathrm{cm^{-1}}$ which is excited by the CO_2 laser. It is assumed that the number of dissociated CH_3OH molecules is proportional to the LIF signal from OH (see Sec. III C). Experiments have been performed with two different CO_2 laser pulses, as discussed in Sec. II, which are characterized by different peak intensities at the same fluence.

As the vibrational density of states for CH_3OH at lower excitation levels is small, a significant nonlinear intensity effect is expected for IR multiphoton excitation from the vibrational ground state and from the lower pre-excitation levels.[30] In Fig. 8 the LIF signal detected from OH is shown for the two different laser pulse shapes as a function of CO_2 laser fluence F. Without pre-excitation the measured LIF signal for the multimode pulse is roughly three times stronger than the signal from the single mode pulse. Pre-excitation to the $v_{OH}=1$ level results in an increase of the measured LIF signal by more than an order of magnitude. In addition, the ratio of the signals from the single mode and multimode pulse is much closer to one than with $v_{OH}=0$.

The dissociation yields F_P[34] for CH_3OH being preexcited to $v_{OH}=3$ and $v_{OH}=5$ are shown in Fig. 9. For the preexcitation to $v_{OH}=3$ and $v_{OH}=5$ a saturation of the measured LIF signal is found for a CO_2 laser fluence larger than the saturation fluence $F_S=50\ \mathrm{J\,cm^{-2}}$ for $v_{OH}=3$ and $F_S=40\ \mathrm{J\,cm^{-2}}$ for $v_{OH}=5$ (Fig. 9). Under these conditions it can thus be assumed that all pre-excited CH_3OH molecules in the LIF probe volume are dissociated by the CO_2 laser. Assuming that the ratio of reaction products leading to CH_3+OH reaction channel does not depend on the laser flu-

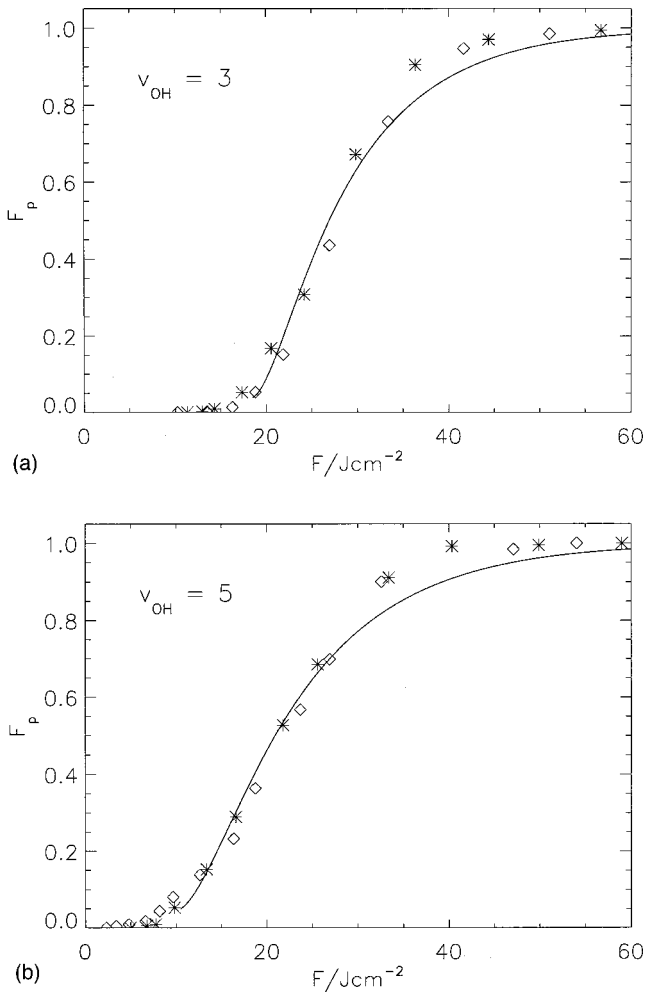

FIG. 9. Experimentally determined IR multiphoton dissociation product yield F_P for CH_3OH preexcited to $v_{OH}=3$ (a) and for $v_{OH}=5$ (b) as function of CO_2 laser fluence F. (*): multimode pulse, ($\diamond$): single mode pulse. The full line represents the result of a fit of Eq. (15) to the experimental data using two exponentials.

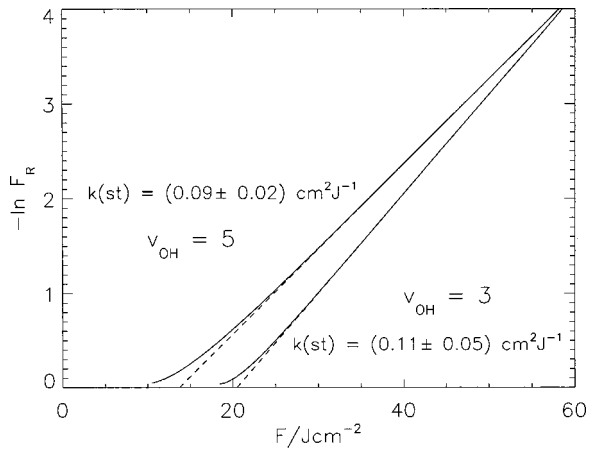

FIG. 10. Logarithmic reactant fluence (LRF) plot of the fit of the model function in Eq. (15) to the experimentally determined dissociation yields $F_P=1-F_R$ from the multiphoton excitation of CH_3OH pre-excited to $v_{OH}=3$ and $v_{OH}=5$ (full line). For two exponential terms in Eq. (15) a steady state rate constant $k_{I3}(\mathrm{st})=(0.105\pm0.053)$ cm^2 J^{-1} is determined for $v_{OH}=3$ and $k_{I5}(\mathrm{st})=0.094\pm0.021$ cm^2 J^{-1} for $v_{OH}=5$. The dashed line represents an extrapolation of the steady-state rate parameter to $F_P=0$ to determine the incubation fluence.

ence between $F=10$ J cm^{-2} and $F=50$ J cm^{-2} (for a discussion of this assumption see Sec. III C), it is possible to calculate true IR multiphoton dissociation yields F_P for the preexcited CH_3OH from the measured LIF signal. For the preexcitation to $v_{OH}=3$ a small difference in the measured product yield F_P at lower laser fluence F for the single mode and multimode laser pulses is still visible [Fig. 9(a)], whereas this difference becomes negligible with preexcitation to $v_{OH}=5$ [Fig. 9(b)].

For the limiting case of a linear intensity dependence of the IR multiphoton excitation process (case B[7,65]), which may be approximately assumed for the pre-excitation to $v_{OH}=3$ and $v_{OH}=5$ (see Sec. III A), the remaining reactant fraction $F_R=C(t)/C_0$ can be described approximately by a sum of exponentials:[34]

$$F_R=1-F_P=\sum_{k=1}\Phi_k\exp(\kappa_k F),\quad \kappa_k<0, \tag{15}$$

where the κ_k are the eigenvalues of the rate coefficient matrix that is used to describe the IR multiphoton excitation process. The steady-state rate constant $k_I(st)$ for the dissociation after IR multiphoton excitation is related to the largest eigenvalue κ_1 (smallest in absolute value)

$$k_I(st)=-\lim_{F\to\infty}\frac{d\ln F_R}{dF}=-\kappa_1. \tag{16}$$

Using two exponentials in the expansion [Eq. (15)], a steady-state rate constant $k_{I3}(st)=0.11\pm0.05$ cm^2 J^{-1} for $v_{OH}=3$ and $k_{I5}(st)=0.09\pm0.02$ cm^2 J^{-1} for $v_{OH}=5$ is determined from a nonlinear fit to the experimental data including two exponential terms. The calculated dissociation yield $F_P(F)$ is given as a solid line in Figs. 9(a) and 9(b) for the two excitation conditions.

The differences in the steady state rate constants with preexcitation to $v_{OH}=3$ and 5 are not significant. However, there is a significant difference in the incubation fluence,[7,34] as expected. This can be seen best from Fig. 10 where we show the two sets of data as logarithmic reactant fluence (LRF) plots.[65] The extrapolation of the linear part ($-\ln F_R^{st}$) of these plots to zero yield ($F_P=0=-\ln F_R^{st}$) provides the incubation fluences which are 20.4 J cm^{-2} for $v_{OH}=3$ and 13.7 J cm^{-2} for $v_{OH}=5$. The physical interpretation of this observation is that more extensive pre-excitation with the NIR laser removes part of the incubation phenomena. Indeed, pre-excitation to about the steady-state average energy of reactant molecules (above the dissociation energy) would remove the incubation fluence completely. Our experimental observations are in qualitative and semiquantitative agreement with the model calculations reported below.

B. Integrated IR absorption intensity for CH_3OH and C_2H_5OH in the spectral region around 1000 cm^{-1}

The efficiency of the IR multiphoton excitation and dissociation process is strongly influenced by three types of quantities:[7,66] The density $\rho(E_M)$ of effectively coupled mo-

TABLE II. Integrated band intensities G for CH_3OH and C_2H_5OH in the spectral region of the CO_2 laser.

Molecule	Normal mode	Range of integration/cm^{-1}	G/pm^2	Reference
CH_3OH	ν_7, ν_8	950–1100	1.71 ± 0.07	This work
CH_3OH	ν_7	[a]	1.69 ± 0.04	70
C_2H_5OH	ν_{14}, ν_{15}, ν_{16}[b]	960–1150	1.64 ± 0.14	This work
	ν_{13}, ν_{15}, ν_{16}[c]			

[a]From integration of single rotational lines.
[b]Anti rotamer according to Ref. 69.
[c]Gauche rotamer according to Ref. 69.

lecular states at the excitation level M, the energy difference between the initial level E_1 and the molecular level E_N where the unimolecular dissociation rate $k(E_N)$ is comparable to the laser driven pumping process, and the electric dipole transition probability of the pumped IR chromophore. The density of molecular states $\rho(E_M)$ is determined by the spectroscopic quantities such as the normal mode frequencies and anharmonic constants of the molecule. The number of CO_2 laser photons which have to be absorbed to reach the dissociation threshold can be calculated from thermochemical or *ab initio* data for the dissociation process. The transition probability between two adjacent levels in IR multiphoton excitation depends on the integrated band strength G of the excited IR chromophore, which is also proportional to the absolute square of the transition moment $|\langle v_f|\mu|v_i\rangle|^2$:[67]

$$G=\frac{1}{Cl}\int_{\text{band}}\ln(I_0/I)d\ln\nu \simeq 41.624\left(\frac{|\langle v_f|\mu|v_i\rangle|^2}{Debye}\right)p\text{m}^2, \quad (17)$$

where C is the number density (in cm^{-3}) of absorbing molecules, l is the optical absorption path length, $I_0(\nu)$ is the incident IR intensity and $I(\nu)$ the transmitted IR intensity. In contrast to the other parameters, the integrated absorption band strength G is frequently not well known. We have measured here the integrated band strength of the C–OH chromophore region in CH_3OH and C_2H_5OH (see Sec. II and Table II).

For CH_3OH, the CO-stretching vibration ν_8 at 1033.5 cm^{-1} and the CH_3-rocking vibration ν_7 at 1074.5 cm^{-1} are the only fundamental vibrations in the spectral region of the emission of the CO_2 laser.[40] The integrated absorption intensity of the ν_7 fundamental is at least one order of magnitude smaller than the one for the CO-stretching vibration (ν_8). In the high resolution spectra, the strong ν_7 rotational lines are still dominated by the absorption of the wings of the ν_8 fundamental vibration, and the contribution of the two overlapping normal modes to the total integrated band intensity cannot be simply separated by integration. Thus, we determined only the sum of the integrated band intensities for the two overlapping bands. The contribution of the ν_7 normal mode to the integrated band intensity G is on the order of the experimental uncertainty, and the efficiency of the IR multiphoton excitation is dominated by the CO-stretching vibration.

We have also studied C_2H_5OH for comparison in order to characterize further the C–OH chromophore for IR multiphoton excitation. $G_{\text{C–OH}}$ is very similar in both alcohols, demonstrating the usefulness of the IR-chromophore concept,[68] if one extends the integration over a large spectral range. In any case, at high excitation, transition probabilities for fundamentals of several chromophores might contribute to the multiphoton process. For both conformers of C_2H_5OH, three overlapping bands contribute to the total integrated band strength in the spectral region around 1050 cm^{-1},[69] and the contribution of the CO-stretching vibration is less dominant for C_2H_5OH than for CH_3OH. Apart from the CO-stretching vibration the other normal modes show a high contribution of CC-stretching and COH-bending character. As it is not possible to separate the contributions from the different vibrational bands to the overall integrated absorption intensity, there is some ambiguity in the exact assignment of the vibrational band strength of the excited chromophore. In our model calculations (see Sec. IV E), the total integrated absorption band strength around 1050 cm^{-1} is used. This may lead to an overestimation for the calculated efficiency of the IR multiphoton excitation for C_2H_5OH. From the *ab initio* calculations of Ref. 69, it may be deduced that the CO-stretching vibration contributes 60% for the anti-rotamer and 80% for the gauche rotamer to the integrated absorption band strength around 1050 cm^{-1}.

The experimental integrated band strengths for CH_3OH and C_2H_5OH in the spectral region around 1050 cm^{-1} are summarized in Table II together with the normal mode assignments and the spectral range for the integration. To our knowledge only the integrated band strength for the CO-stretching vibration of CH_3OH has been determined previously.[70] In spite of very different experimental approaches, the results agree well.

C. Master equation calculations for the IR multiphoton excitation of CH_3OH from the vibrational ground state and pre-excited to $\nu_{OH}=1$

Our experiments reveal a significant nonlinear intensity effect for the multiphoton excitation of CH_3OH from the vibrational ground state. Case B/C master equation calculations have been performed for the excitation from the vibrational ground state for the three laser pulses shown in Fig. 3. The results of the calculation are shown in Fig. 11(a) together with the experimental data points. The measured LIF signals have been scaled to the calculated results for the dissociation yield F_P with the single mode pulse in order to allow for presentation in the same figure. This implies a scaling factor $f_{sc}=10^{-6}$, and allows for comparison of product yield relative to other pulse shapes, using the same scaling factor. Only when saturation in dissociation is reached can one determine yields absolutely from the LIF signal. The experimental results for the multimode pulse are found, as expected, between the calculated yields for the two ''extreme'' multimode pulses of Fig. 3. Comparing the calculated results for the two different multimode pulses one can conclude that a high percentage of ideally locked (identical

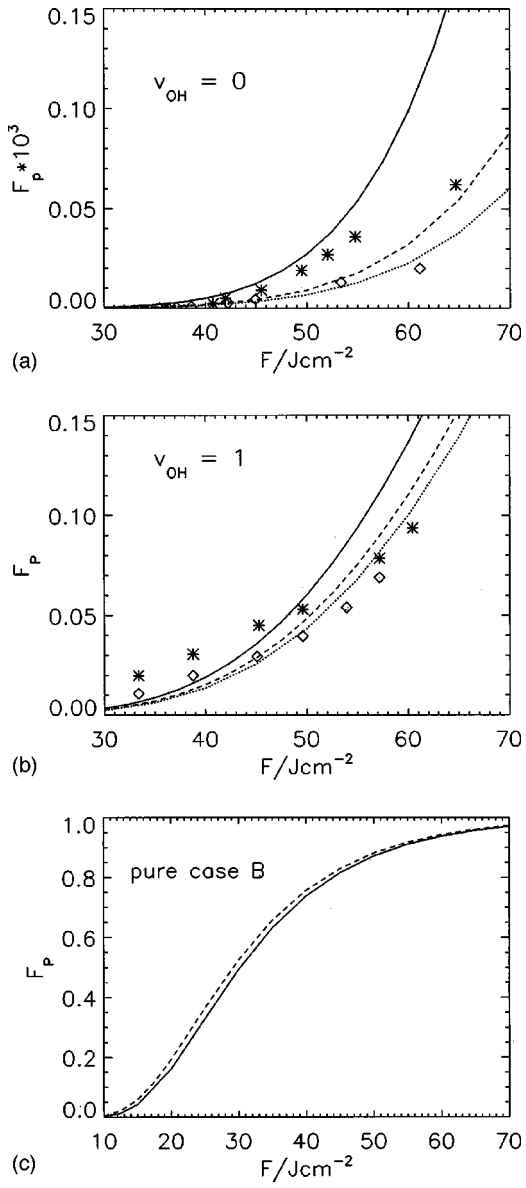

FIG. 11. (a) Case B/C calculated dissociation yields F_P for IR multiphoton dissociation of CH_3OH from the vibrational ground state for the three different laser pulses of Fig. 3. (——): Multimode pulse with "ideal" phase relations, (— — —): multimode pulse with modest phase relation, (· · · ·): single mode pulse. Also included are the experimental dissociation yields using a scaling factor $f_{sc}=1\cdot10^{-6}$ (*): multimode pulse, (◇): single mode pulse. (b) Case B/C calculated dissociation yields F_P for IR multiphoton dissociation of CH_3OH pre-excited to $v_{OH}=1$ for the three different laser pulses of Fig. 3. (——): multimode pulse with "ideal" phase relations (— — —), multimode pulse with modest phase relation (· · · ·): single mode pulse. Also included are the experimental dissociation yields using a scaling factor $f_{sc}=3\cdot10^{-4}$ (*): multimode pulse, (◇): single mode pulse. (c) Calculated dissociation probability of CH_3OH from the vibrational ground state (——) and pre-excited to $v_{OH}=1$ (— — —) using a pure case B master equation.

phase for many resonator modes) is desirable to study nonlinear intensity effects in IR multiphoton excitation experiments in more detail.

The experiments using pre-excitation of CH_3OH to $v_{OH}=1$ [Fig. 11(b)] show a reduced nonlinear intensity effect compared to the experiments from the vibrational ground state [Fig. 11(a)]. Again the experimental results for the measured LIF signal with excitation by the single mode pulse has been scaled to the calculated dissociation yields F_P (with $f_{sc}=3\times10^{-4}$), in order to allow for presentation of experimental and theoretical results in the same figure on a similar scale. As fewer steps, where a case C master equation is applicable, are important with pre-excitation to $v_{OH}=1$, the calculations show a less pronounced nonlinear intensity effect in agreement with the smaller experimental effect.

A note may be useful on the magnitude of the scaling factor, which is significantly larger with pre-excitation to $v_{OH}=1$ than with excitation from the vibrational ground state. Two effects have to be considered to explain this increase of the scaling factor. Only a small fraction of the ground-state CH_3OH molecules are excited to $v_{OH}=1$ with the near IR laser which would reduce the actually measured LIF signal at least by 2 orders of magnitude. But a second effect will lead to a contribution in the opposite direction. As explained in Sec. IV A, the experiments are performed with a large off-resonance shift of nearly 100 cm^{-1}. The molecules are irradiated with 10P20 CO_2 laser line at 944.194 cm^{-1}, whereas the ν_8 fundamental of CH_3OH is found at 1033.5 cm^{-1}. For the pre-excitation to $v_{OH}=1$, a shift of the measured IR spectra in the region of the CO-stretching vibration is generally assumed, which leads to an additional increase of the IR multiphoton excitation efficiency for CH_3OH at 944 cm^{-1} compared to the excitation from the vibrational ground state.

For pure case B master equation calculations, a significant dissociation yield is obtained for the IR multiphoton excitation of CH_3OH from the vibrational ground state already at laser fluence of $F=15\ J\,cm^{-2}$. For a fluence larger than 60 $J\,cm^{-2}$, more than 90% of the CH_3OH molecules are dissociated. The dissociation is slightly more efficient for molecules pre-excited to $v_{OH}=1$ since the number of IR photons which have to be absorbed is lower. The calculated dissociation yields assuming a pure case B (linear intensity dependence) for CH_3OH from the vibrational ground state and pre-excited to $v_{OH}=1$ are shown in Fig. 11(c). These hypothetical yields are much larger than in case B/C calculations.

D. Master equation calculations for the IR multiphoton excitation of CH_3OH pre-excited to $v_{OH}=3$ and $v_{OH}=5$

No pronounced difference for the two laser pulse types was found for the measured IR multiphoton dissociation yield of CH_3OH pre-excited to $v_{OH}=3$ and $v_{OH}=5$, in agreement with the predictions of case B/C master equation calculations. A pure case B master equation gives a slightly higher dissociation probability for $v_{OH}=3$ compared to case B/C calculations, where nonlinear intensity corrections are included [Fig. 12(a)]. The difference is more pronounced at lower laser fluences (and intensities), since case C effects are more important for lower laser intensities. In the experiments the difference of a factor of 2–2.5 in the peak intensity for the two laser pulses (see Fig. 3) is too small to allow us to measure this effect. Laser pulses with a larger intensity ratio are needed to investigate nonlinear intensity effects in the close transition regime from a case B/C to a pure case B description. There is a small nonlinear intensity effect visible

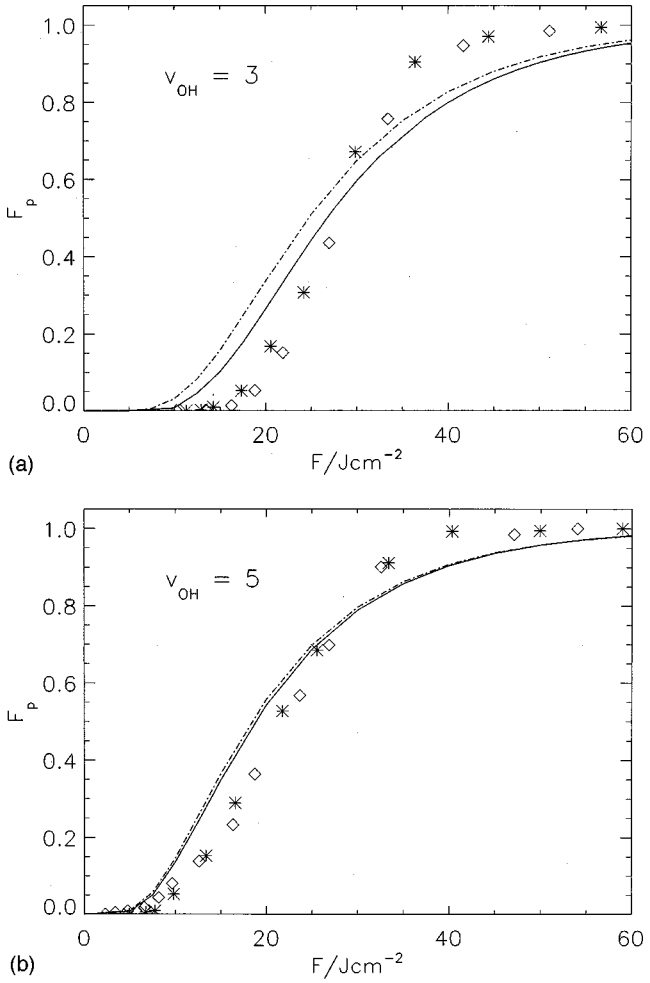

FIG. 12. Calculated dissociation yields F_P for the IR multiphoton excitation of CH_3OH pre-excited to $v_{OH}=3$ (a) and for $v_{OH}=5$ (b). (——): case B/C master equation—results for single mode and multimode laser pulse coincident, (—·—·—·—): pure case B master equation. Also included are experimental dissociation yields for multimode (*) and single mode (◇) laser pulses.

in the experiment, but it is still within the uncertainty of the measurements. Only a minor difference for the calculated dissociation yields for a case B/C and a pure case B master equation could be found for $v_{OH}=5$ [Fig. 12(b)].

For the pre-excitation of CH_3OH to $v_{OH}=3$ and $v_{OH}=5$, the measured LIF signal could be translated into absolute dissociation yields F_P (see Sec. IV A). The experimental dissociation yields for $v_{OH}=3$ were used to adjust the bandwidth parameter $\Delta\nu$ in Eq. (3). A value of $\Delta\nu=325\ \mathrm{cm}^{-1}$ has been used in the calculations for all the pre-excitation conditions. A perfect agreement between the measured and calculated dissociation yields F_P is obtained for the IR multiphoton excitation of CH_3OH preexcited to $v_{OH}=5$ using the bandwidth parameter adjusted for $v_{OH}=3$. For excitation with a constant laser intensity of 100 MW cm^{-2}, a steady-state rate constant $k_{I3}(st)=0.075\ \mathrm{J}^{-1}\,\mathrm{cm}^2$ for $v_{OH}=3$ and $k_{I5}(st)=0.082\ \mathrm{J}^{-1}\,\mathrm{cm}^2$ for $v_{OH}=5$ is derived from a case B/C master equation. Both calculated steady-state rate constants are in good agreement with the values from the fit of an exponential expansion [Eq. (15)] to the measured dissociation yields (see Sec. IV A) within the experimental uncertainty.

The calculated dissociation yields F_P for the IR multiphoton dissociation of CH_3OH pre-excited to $v_{OH}=3$ and to $v_{OH}=5$ using a case B/C and a pure case B master equation are shown together with the experimental results in Fig. 12. For both pre-excitations the fluence dependence of the experimental dissociation yields are significantly steeper than calculated, particularly so for $v_{OH}=3$. This can be explained at least in part by the crude modeling of rate coefficients $K_{M,M+1}$ in our master equation treatment. In order to improve upon this, more information than presently available would be needed on the spectroscopy of highly excited CH_3OH. Secondly, the detailed spatial fluence distribution in the excitation region of the experiments would have to be modeled more closely (at substantial additional expense). At the present level of accuracy of the model calculations, the agreement can be considered satisfactory, particularly as far as the very large increases in dissociation yield with pre-excitations going from $v_{OH}=3$ to $v_{OH}=5$ are concerned.

E. Master equation calculations for the IR multiphoton excitation of C_2H_5OH from the vibrational ground state

It is of some interest to extend our calculations to predict the IR multiphoton excitation and dissociation of ethanol

$$C_2H_5OH \xrightarrow{nh\nu} C_2H_4+H_2O \quad \mathbf{E}_o=281\ \mathrm{kJ\,mol}^{-1}. \tag{18}$$

Although there has been some controversy concerning the details of the thermal decomposition of C_2H_5OH,[71] the early assumption that the lowest dissociation channel leads to $C_2H_4+H_2O$ has been confirmed recently in experiments with chemically activated ethanol and by *ab initio* calculations.[72] In these calculations, the transition state for the H_2O elimination channel was found to be 23 500 cm^{-1} above the ground state. The dissociation energies for breaking the CC-bond ($D_0=29\,600\ \mathrm{cm}^{-1}$) and the CO-bond ($D_0=32\,100\ \mathrm{cm}^{-1}$) are significantly higher than this value. RRKM calculations[72] show that the dissociation process for an excitation energy up to 35 000 cm^{-1} is still dominated by the lowest reaction channel. The other reaction channels become important only at higher excitation energies due to their larger pre-exponential factor A_∞. In our master equation calculation for the IR multiphoton excitation of C_2H_5OH only the lowest reaction channel leading to $C_2H_4+H_2O$ has been considered, and the vibrational frequencies to calculate the densities of states for the reactant and the transition state are taken from Ref. 72. To calculate the up-pumping rate in Eq. (3), the total integrated band strength G in the spectral range between 960 and 1150 cm^{-1} from Table II has been used. From the calculated density of states for C_2H_5OH, one can see that for laser intensities above 250 MW cm^{-2} only the lowest 3 to 4 levels show a transition to a case C behavior. Therefore, only a weak nonlinear intensity effect is expected for the IR multiphoton excitation process of C_2H_5OH.

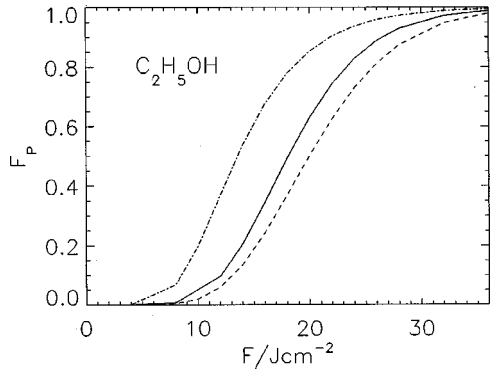

FIG. 13. Calculated IR multiphoton dissociation yields for C_2H_5OH from the vibrational ground state. (——): multimode laser pulse, case B/C, (· · · ·): single mode laser pulse, case B/C, (—·—·—·—): pure case B.

The calculated dissociation yields F_P for the IR multiphoton excitation of C_2H_5OH are shown in Fig. 13. The efficiency of the excitation process is comparable or slightly higher than the excitation of CH_3OH pre-excited to $v_{OH}=5$. Comparing the calculated results using a case B/C master equation for the ideally locked multimode pulse with those for the single mode pulse reveals a small but significant nonlinear intensity effect. As for CH_3OH pre-excited to $v_{OH}=3$ a significant increase in the calculated dissociation yields is found if a pure case B master equation is applied. These predictions are in good qualitative agreement with expectations resulting from the reduced dissociation threshold energy for C_2H_5OH compared to CH_3OH and with the higher density of states for the former. Thus, we predict that IR multiphoton excitation and dissociation of ethanol at room temperature should be far easier than for methanol. The assumed dissociation channel leading to H_2O and C_2H_4 has been confirmed in IR multiphoton excitation experiments of C_2H_5OH.[73,74] To our knowledge a deconvoluted dependence of product yields F_P upon laser fluence has not yet been published. It would be possible to detect ethylene products by direct IR absorption.[75–77]

V. CONCLUSIONS

The present, combined experimental and theoretical investigation has shown that the methanol molecule offers rich opportunities to study fundamental aspects of IR multiphoton excitation and dissociation.

We can draw in this context the following main conclusions:

(i) The simple bond fission reaction leading to CH_3+OH is a major dissociation channel, and LIF detection of OH can be used to study total dissociation yields as a function of IR-laser parameters;

(ii) the infrared multiphoton excitation without pre-excitation ($v_{OH}=0$) and with modest pre-excitation ($v_{OH}=1$, to some extent also $v_{OH}=3$) shows strong nonlinear intensity effects as revealed by the use of different laser pulse shapes. In contrast to this, pre-excitation to $v_{OH}=5$ removes the nonlinear intensity dependence almost completely;

(iii) quantitative case B/C master equation calculations of the IR multiphoton excitation of methanol are able to reproduce well the nonlinear intensity effects. Calculated and experimental steady-state coefficients agree well, and the changes of incubation fluences with different pre-excitation are predicted quantitatively;

(iv) the experimental and theoretical analysis demonstrates conclusively that for a relatively small molecule such as CH_3OH, the nonlinear intensity dependence characterized by the case B/C master equation is an important, even dominant contribution to the selectivity necessary for IRLAPS;

(v) extension of the calculations to C_2H_5OH predict a substantial decrease of nonlinear intensity effects, with greatly increased efficiency of IR multiphoton excitation and dissociation.

Methanol is thus an interesting test molecule for infrared multiphoton excitation, in the intermediate size range, where full quantum dynamical simulations are currently impossible, but where nonlinear intensity effects are important and a simple ''linear'' case B master equation would be inappropriate. Because of its great spectroscopic interest[40,70] and its role as a test case for the interplay of large amplitude motions and intramolecular vibrational redistribution[23,46,78–81] further study at even greater detail would be warranted. However, even at the present, still rather crude level, we find numerous important implications for understanding the reaction dynamics of methanol, with applications ranging from atmospheric chemistry to combustion, for infrared multiphoton excitation in general, and for selectivity in IRLAPS and one- or two-frequency laser isotope separation with polyatomic molecules.

ACKNOWLEDGMENTS

Our work is supported financially by EPF Lausanne and ETH Zürich (including C^4, AGS and CSCS projects) as well as by the Schweizerischer Nationalfonds through Grant Nos. 20-59261.99, 20-58985.99, and 2000-066982.01/1. We gratefully acknowledge also helpful discussions with Michael Hippler, Hans Hollenstein, David Luckhaus, Roberto Marquardt, Jürgen Stohner, and Martin Willeke.

[1] M. Göppert-Mayer, Ann. Phys. **9**, 273 (1931); M. Göppert, Naturwissenschaften **17**, 932 (1929).
[2] J. H. Shirley, Phys. Rev. B **138**, 979 (1965).
[3] W. Kaiser and C. G. B. Garrett, Phys. Rev. Lett. **7**, 229 (1961).
[4] M. Quack, Multiphoton Excitation, in *Encyclopedia of Computational Chemistry, Vol. 3*, edited by P. V. Ragué Schleyer, N. Allinger, T. Clark, J. Gasteiger, P. A. Kollman, H. F. Schaefer III, and P. R. Schreiner (Wiley, New York, 1998), pp. 1775–1791.
[5] E. R. Grant, P. A. Schulz, A. S. Sudbæ, Y. R. Shen, and Y. T. Lee, Phys. Rev. Lett. **40**, 115 (1978).
[6] N. Bloembergen and E. Yablonovitch, Phys. Today **31**, 23 (1978).
[7] M. Quack, J. Chem. Phys. **69**, 1282 (1978).
[8] M. N. R. Ashfold, G. Hancock, and G. Ketley, Faraday Discuss. Chem. Soc. **67**, 204 (1979).
[9] D. S. King and J. C. Stephenson, Chem. Phys. Lett. **66**, 33 (1979).
[10] M. Rossi, J. R. Barker, and D. M. Golden, Chem. Phys. Lett. **65**, 523 (1979).
[11] M. Quack, P. Humbert, and H. Van Den Bergh, J. Chem. Phys. **73**, 247 (1980).
[12] M. Quack and G. Seyfang, Chem. Phys. Lett. **93**, 442 (1982).

[13] M. Quack, E. Sutcliffe, P. A. Hackett, and D. M. Rayner, Faraday Discuss. Chem. Soc. **82**, 229 (1986).
[14] M. Quack, R. Schwarz, and G. Seyfang, J. Chem. Phys. **96**, 8727 (1992).
[15] Y. He, J. Pochert, M. Quack, R. Ranz, and G. Seyfang, J. Chem. Soc. Faraday Discuss. **102**, 275 (1995).
[16] M. Quack and E. Sutcliffe, QCPE Bulletin **6**, 98 (1986).
[17] R. Marquardt, M. Quack, and J. Stohner, QCPE (to be published).
[18] P. Dietrich, M. Quack, and G. Seyfang, QCPE (to be published).
[19] D. W. Lupo and M. Quack, Chem. Rev. **87**, 181 (1987).
[20] M. Quack, Infrared Phys. **29**, 441 (1989).
[21] R. D. F. Settle and T. R. Rizzo, J. Chem. Phys. **97**, 2823 (1992).
[22] O. V. Boyarkin, R. D. F. Settle, and T. R. Rizzo, Ber. Bunsenges. Phys. Chem. **95**, 504 (1995).
[23] L. Lubich, O. V. Boyarkin, R. D. F. Settle, D. S. Perry, and T. R. Rizzo, Faraday Discuss. Chem. Soc. **102**, 167 (1995).
[24] M. Quack, Infrared Phys. Technol. **36**, 365 (1995).
[25] C. S. Parmenter, Faraday Discuss. Chem. Soc. **75**, 7 (1983), M. Quack, Philos. Trans. R. Soc. London, Ser. A **332**, 203 (1990); K. K. Lehmann, G. Scoles, B. Pate, Annu. Rev. Phys. Chem. **45**, 241 (1994); M. Quack and W. Kutzelnigg, Ber. Bunsenges. Phys. Chem. **99**, 231 (1995); D. J. Nesbitt and R. W. Field, J. Phys. Chem. **100**, 12735 (1996); R. Marquardt and M. Quack, Energy redistribution in reacting systems, in *Encyclopedia of Chemical Physics and Physical Chemistry, Vol. 1 (Fundamentals)*, edited by J. H. Moore and N. D. Spencer (IOP, Bristol, 2001), Chap. A 3.13, pp. 653–682, and further references cited therein.
[26] O. V. Boyarkin, M. Kowalczyk, and T. R. Rizzo (in preparation).
[27] O. V. Boyarkin and T. R. Rizzo, J. Chem. Phys. **105**, 6285 (1996).
[28] G. H. Dieke and H. M. Crosswhite, J. Quant. Spectrosc. Radiat. Transf. **2**, 97 (1962).
[29] M. Quack, C. Ruede, and G. Seyfang, Spectrochim. Acta, Part A **46**, 523 (1990).
[30] M. Quack, Adv. Chem. Phys. **50**, 395 (1982).
[31] M. Quack and E. Suttcliffe, Chem. Phys. Lett. **99**, 167 (1983), **105**, 147 (1984).
[32] M. Quack and E. Sutcliffe, J. Chem. Phys. **83**, 3805 (1985).
[33] S. Hervé, F. Le Quéré, and R. Marquardt, J. Chem. Phys. **114**, 826 (2001).
[34] M. Quack, Ber. Bunsenges. Phys. Chem. **83**, 757 (1979).
[35] M. Quack, Ber. Bunsenges. Phys. Chem. **85**, 318 (1981).
[36] M. Quack and J. Troe, Statistical Adiabatic Channel Model, in *Encyclopedia of Computational Chemistry, Vol. 4*, edited by P. V. Ragué Schleyer, N. Allinger, T. Clark, J. Gasteiger, P. A. Kollman, H. F. Schaefer III, and P. R. Schreiner (Wiley, New York, 1998), pp. 2708–2726.
[37] T. Beyer and D. F. Swinehart, Commun. ACM **16**, 379 (1973).
[38] S. E. Stein and B. S. Rabinovitch, J. Chem. Phys. **59**, 2438 (1973).
[39] M. Quack, J. Phys. Chem. **83**, 150 (1979).
[40] G. Moruzzi, B. P. Winnewisser, M. Winnewisser, I. Mukhopadhyay, and F. Strumia, *Microwave, Infrared, and Laser Transitions in Methanol* (CRC, Boca Raton, 1995).
[41] K. Spindler and H. G. Wagner, Ber. Bunsenges. Phys. Chem. **86**, 2 (1982).
[42] M. Quack and J. Troe, Ber. Bunsenges. Phys. Chem. **78**, 240 (1974).
[43] R. Meyer, J. Chem. Phys. **52**, 2053 (1970).
[44] B. Fehrensen, D. Luckhaus, and M. Quack, Chem. Phys. Lett. **300**, 312 (1999).
[45] D. Luckhaus, J. Chem. Phys. **113**, 1329 (2000).
[46] B. Fehrensen, D. Luckhaus, M. Quack, M. Willeke, and T. R. Rizzo (in preparation).
[47] Z. Bačić and J. C. Light, Annu. Rev. Phys. Chem. **40**, 469 (1989).
[48] O. V. Boyarkin, T. R. Rizzo, and D. S. Perry, J. Chem. Phys. **110**, 11359 (1999); D. Rueda, O. V. Boyarkin, T. R. Rizzo, I. Mukhopahyay, and D. S. Perry, J. Chem. Phys. **116**, 91 (2002).
[49] L. H. Xu and J. T. Hougen, J. Mol. Spectrosc. **173**, 540 (1995).
[50] S. A. Bialkowski and W. A. Guillory, Chem. Phys. **67**, 2061 (1977).
[51] R. Schmiedl, U. Meier, and K. H. Welge, Chem. Phys. Lett. **80**, 495 (1981).
[52] C. W. Bauschlicher, S. R. Langhoff, and S. P. Walch, J. Chem. Phys. **96**, 450 (1992).
[53] S. P. Walch, J. Chem. Phys. **98**, 3163 (1993).
[54] M. W. Chase, Jr., *NIST-JANAF Thermochemical Tables*, J. Phys. Chem. Ref. Data, 1998.
[55] M. Quack, The Role of Intramolecular Coupling and Relaxation in IR-Photochemistry, in *Intramolecular Dynamics*, edited by J. Jortner and B. Pullman, pp. 371–390, (D. Reidel Publishing Company, Dordrecht, 1982), pp. 371–390, Proceedings of the Fifteenth Jerusalem Symposium on Quantum Chemistry and Biochemistry Held in Jerusalem, Israel, March 29–April 1, 1982.
[56] W. Hack and H. Thiesemann, J. Phys. Chem. **99**, 17364 (1995).
[57] J. J. Lin, J. Shu, Y. T. Lee, and X. Yang, J. Chem. Phys. **113**, 5287 (2000).
[58] C. C. Miller, R. D. Van Zee, and J. C. Stephenson, J. Chem. Phys. **114**, 1214 (2001).
[59] R. Humpfer, H. Oser, and H. Grotheer, Int. J. Chem. Kinet. **27**, 577 (1995).
[60] M. Brouard, H. M. Lambert, C. L. Russell, J. Short, and J. P. Simons, Faraday Discuss. Chem. Soc. **102**, 179 (1995).
[61] W. Hack, Faraday Discuss. Chem. Soc. **102**, 260 (1995).
[62] M. Quack, Faraday Discuss. Chem. Soc. **102**, 260 (1995).
[63] M. Quack and J. Troe, Ber. Bunsenges. Phys. Chem. **79**, 469 (1975).
[64] J. R. Beresford, G. Hancock, A. J. MacRobert, J. Catanzarite, G. Radakrishnan, H. Reisler, and C. Wittig, Faraday Discuss. Chem. Soc. **75**, 211 (1983).
[65] M. Quack, J. Chem. Phys. **70**, 1069 (1979).
[66] M. Quack, Ber. Bunsenges. Phys. Chem. **83**, 1287 (1979).
[67] M. Quack, Annu. Rev. Phys. Chem. **41**, 839 (1990).
[68] M. Quack and H. J. Thöne, Ber. Bunsenges. Phys. Chem. **87**, 582 (1983).
[69] R. A. Shaw, H. Wieser, R. Dutler, and A. Rauk, J. Am. Chem. Soc. **112**, 5401 (1990).
[70] M. Dang-Nhu, G. Blanquet, J. Walrand, M. Allegrini, and G. Moruzzi, J. Mol. Spectrosc. **141**, 348 (1990).
[71] W. Tsang, Int. J. Chem. Kinet. **8**, 193 (1976); J. Phys. Chem. Ref. Data **16**, 471 (1987).
[72] N. I. Butkovskaya, Y. Zhao, and D. W. Setser, J. Phys. Chem. **98**, 10779 (1994).
[73] G. P. Zhitneva, High Energy Chem. **20**, 372 (1986).
[74] R. A. Back, D. K. Evans, R. D. McAlpine, E. M. Verpoorte, M. Ivanco, J. W. Goodale, and H. M. Adams, Can. J. Chem. **66**, 857 (1988).
[75] H. Gross, Y. He, M. Quack, A. Schmid, and G. Seyfang, Chem. Phys. Lett. **213**, 122 (1993).
[76] H. Gross, Y. He, M. Quack, and G. Seyfang, in *Springer Proceedings in Physics, Vol. 74, Time-Resolved Vibrational Spectroscopy VI*, edited by A. Lau, F. Siebert, and W. Werncke (Springer-Verlag, Berlin Heidelberg, 1994), pp. 169–172.
[77] H. Gross, Y. He, C. Jeitziner, M. Quack, and G. Seyfang, Ber. Bunsenges. Phys. Chem. **99**, 358 (1995).
[78] O. V. Boyarkin, L. Lubich, R. D. F. Settle, D. S. Perry, and T. R. Rizzo, J. Chem. Phys. **107**, 8409 (1997).
[79] M. Quack, Faraday Discuss. Chem. Soc. **102**, 245 (1995); **102**, 253 (1995).
[80] T. R. Rizzo, Faraday Discuss. Chem. Soc. **102**, 251 (1995).
[81] M. Quack and M. Willeke, J. Chem. Phys. **110**, 11958 (1999).
[82] P. R. Bunker, P. Jensen, W. P. Kraemer, and R. Beardsworth, J. Phys. Chem. **85**, 3724 (1986).
[83] B. Ruscic and J. Berkowitz, J. Phys. Chem. **97**, 11451 (1993).
[84] B. Ruscic and J. Berkowitz, J. Chem. Phys. **95**, 4033 (1991).
[85] D. D. Wagman, W. E. Evans, V. B. Parker, R. H. Schumm, I. Halow, S. M. Bailey, K. L. Churney, and R. L. Nutall, J. Phys. Chem. Ref. Data **11**, Suppl. 2, 84 (1982).
[86] J. D. Goddard and H. F. I. Schaefer, J. Chem. Phys. **70**, 5117 (1979).